

## Study of the different ceramic additions effect on the 316L morphological properties during attrition milling

Haroune Rachid Ben Zine <sup>1,2</sup>, Csaba Balázs <sup>2</sup>, Katalin Balázs <sup>2</sup>

<sup>1</sup>*Doctoral School of Materials Science and Technologies, Óbuda University, Bécsi str. 96/B, Budapest, Hungary*

<sup>2</sup>*Centre for Energy Research, Hungarian Academy of Sciences, Konkoly-Thege M. str. 29-33, Budapest, Hungary*

### Abstract

The effect of the 0.33 and 1 wt% ceramics addition to the 316L Stainless Steel (SS) morphological properties during the attrition milling have been studied. Commercial Höganäs 316L Stainless Steel (SS) powder with additions consisting of the submicron SiC, Si<sub>3</sub>N<sub>4</sub> and Y<sub>2</sub>O<sub>3</sub> ceramic powders have been investigated in present paper. Six different powder mixtures have been prepared with the compositions of 316L/0.33wt% and 316L/1wt% of the ceramic addition. Enhanced morphological changes and homogenous distribution of the ceramic particles in the steel matrix have been achieved in most of the cases.

**Keywords:** CDS steel, Attrition Milling, Morphological study

### 1. Introduction

Mechanical alloying (MA) is attracting for researchers due to its unique advantages and large scale availability. Ni-based oxide dispersion strengthened (ODS) steels have been developed by this technique in early 1960s [1]. *H. Oka et al* studied the effect of milling process and alloying additions on oxide particle dispersion in austenitic stainless steel in order to understand the minor alloying elements on the dispersoids distribution [2]. They found that 6 hours are enough to disperse the Y<sub>2</sub>O<sub>3</sub> in the steel matrix, also it was found that the usage of 0.2–0.3 wt% Zr or 0.6 wt% Hf increases the hardness of the steel by improving the finer oxides distribution in the matrix. Ball milling can be used to obtain nano-sized grains, this refinement of the grains size increased the composites hardness despite the formation of the oxides. The potential of the pitting corrosion has been decreased due to the presence of submicronic grains [3]. *B.Al Mangour et al* investigated the in situ formation of TiC-particle-reinforced stainless steel matrix nanocomposites during ball milling up to 35 hours [4]. During prolonged mechanical alloying, it was observed that the grains are just flattened after 10h, become larger (coarsening) after up to 24h and the grains refinement took place at the end of the process. The final powder mixture was a nanocomposite with homogeneously

dispersed TiC particles. It has been found that 5 hours of milling provides better interface in the case of 316L-50 tungsten (W) comparing to 10hours milling. The interface formation in the case of 316L-50W/W showed uncompleted reaction which is related to the presence of residual pores. Also, it has been found that the excessive milling decreases the joint homogeneity and it is insufficient for graded interfaces [5, 6]. In their study about the effect of surface enriched chromium and grain refinement by ball milling on corrosion resistance of 316L stainless steel. *L. Jinlong et al* showed that it is possible to enrich grains surface of the 316L stainless steel during the ball milling process which will improve the corrosion resistance by cancelling the negative influence of the  $\alpha'$ -martensite [7]. The attrition milling provides higher milling efficiency in much shorter time comparing to the conventional ball milling process.

The aim of this study is to provide better understanding of the effect of different ceramic addition on the efficiency of the attrition milling and to the 316L stainless steel powder morphology during milling.

## 2. Experimental Procedure

The submicron SiC (H.C. Starck), Si<sub>3</sub>N<sub>4</sub> (UBE, SN-ESP) and Y<sub>2</sub>O<sub>3</sub> (H.C. Starck, grade C) have been used as additives to the commercial 316L SS from Höganäs to prepare Ceramic Dispersion Strengthened Steel (CDS) with the following composition: 316L/0.33 wt% and 316L/1 wt% ceramic addition (Tab. 1). The globular 316L has an average grains size of ~70 $\mu$ m with the presence of satellites (Fig. 1A). The composition of the 316L/ceramic powder mixtures is shown in Tab. 1.

Additions (wt%)	0.33 wt% Y <sub>2</sub> O <sub>3</sub>	1 wt% Y <sub>2</sub> O <sub>3</sub>	0.33 wt% SiC	1 wt% SiC	0.33 wt% Si <sub>3</sub> N <sub>4</sub>	1 wt% Si <sub>3</sub> N <sub>4</sub>
316L	1	1	1	1	1	1

**Tab. 1.** Summary of the compositions of the 316L/ceramic powder mixtures

The Union Process attritor mill type 01-HD/HDDM has been used in order to reduce the steel grains size and insure a homogeneous distribution of the ceramic particles in the steel matrix. The composites have been milled in ethanol for 5 hours at 600 rpm. The structure and morphology of the milled powders have been investigated using the scanning electron microscopy (SEM, Zeiss-SMT LEO 1540 XB and Jeol JSM-25-SIII) equipped with EDS. The X-ray diffractometer Bruker AXS D8 with CuK $\alpha$  radiation have been used to analyze the Phases in the different composites analyses.

### 3. Results and discussion

#### 3.1. Investigation of the Morphological changes

##### 3.1.1 Milling of the 316L SS without ceramic additions

The 316 SS grains transformed mainly from globular (Fig. 1A) to flattened and flake-like shape with the presence of few slightly damaged grains after 5 hours wet milling in ethanol (Fig. 1B). Some of the thin flake-like grains broke down into the very small particles shown in Fig. 1B. The average grain size increased due to the grains flattening. The milling was not as efficient as we expected most probably due to the simultaneous higher hardness and plasticity shown by particular grains. Therefore the morphology of resulting powder is characterized by both flattened or partially transformed globular shape.

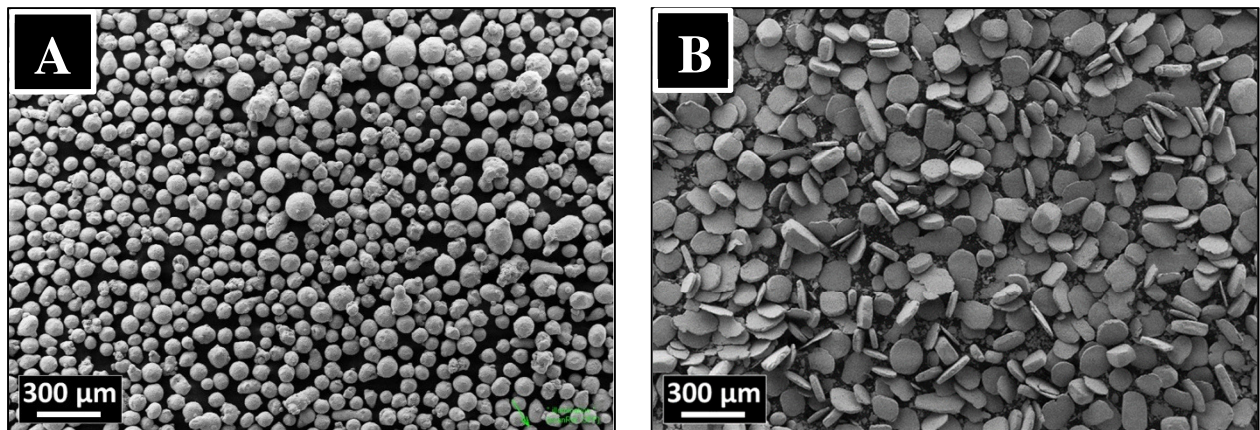


Fig.1. SEM Images of the 316L powder A) Before milling B) After 5 hours milling

##### 3.1.2 Milling of the 316L SS with $Y_2O_3$ addition

Fig. 2A shows the milled 316L/0.33 wt%  $Y_2O_3$  composite, the milling efficiency in this case is higher than for 316L as a higher ratio of the flake-like grains to the flattened grains is observed. In the case of the 316L/1 wt%  $Y_2O_3$  (Fig. 2B) more flattened grains are present which indicates a small decrease in the milling efficiency.

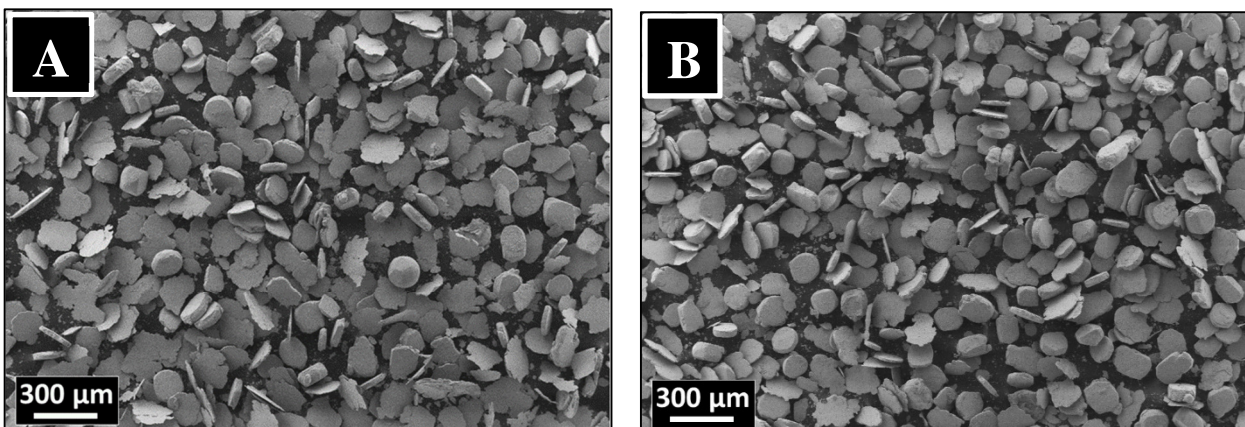


Fig. 2. SEM Images of the milled 316L/ $Y_2O_3$  A) 316L/0.33 wt%  $Y_2O_3$ , B) 316L/1 wt%  $Y_2O_3$

### 3.1.3 Milling of the 316L SS with SiC addition

Total transformations from globular shaped to flake-like shaped grains have been observed in the case of the 316L/0.33 wt% SiC (Fig. 3A). Similar shape transformation and flake-like morphology have been observed in the case of the 316L/1 wt% SiC (Fig. 3B) with the presence of few thicker and larger flake-like shape grains.

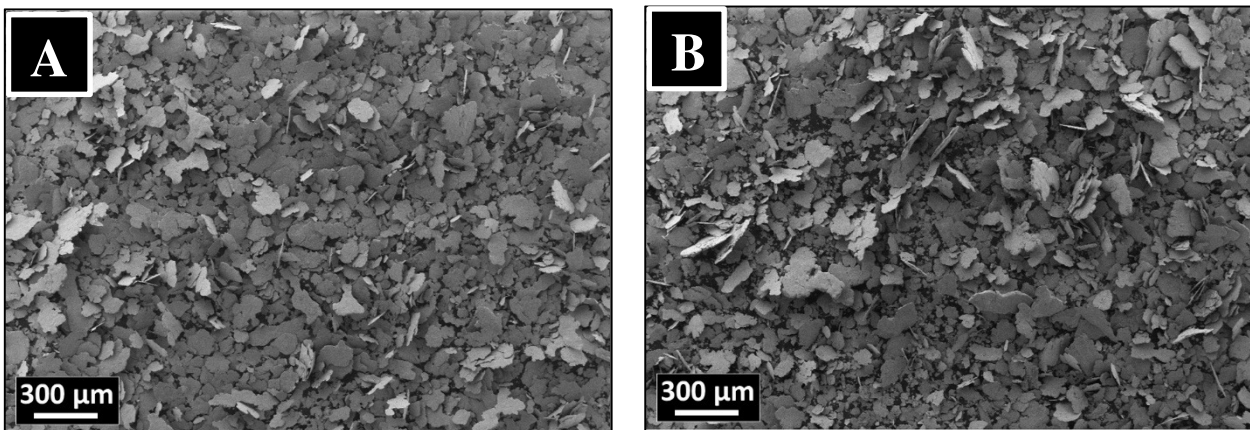


Fig. 3. SEM Images of the milled 316L /SiC, A) 316L/0.33 wt% SiC, B) 316L/1 wt% SiC

### 3.1.4. The milling of the 316L SS with Si<sub>3</sub>N<sub>4</sub> addition

The effect of the Si<sub>3</sub>N<sub>4</sub> on the milling efficiency is very clear, in the case of the 316L/0.33 wt% Si<sub>3</sub>N<sub>4</sub> composite (Fig. 4A) we have a total transformation from globular to flake-like shape grains unlike in the case of the 316L/1 wt% Si<sub>3</sub>N<sub>4</sub> (Fig. 4B) where the majority of the steel grains were just showed flattened morphology with lower transformation grade.

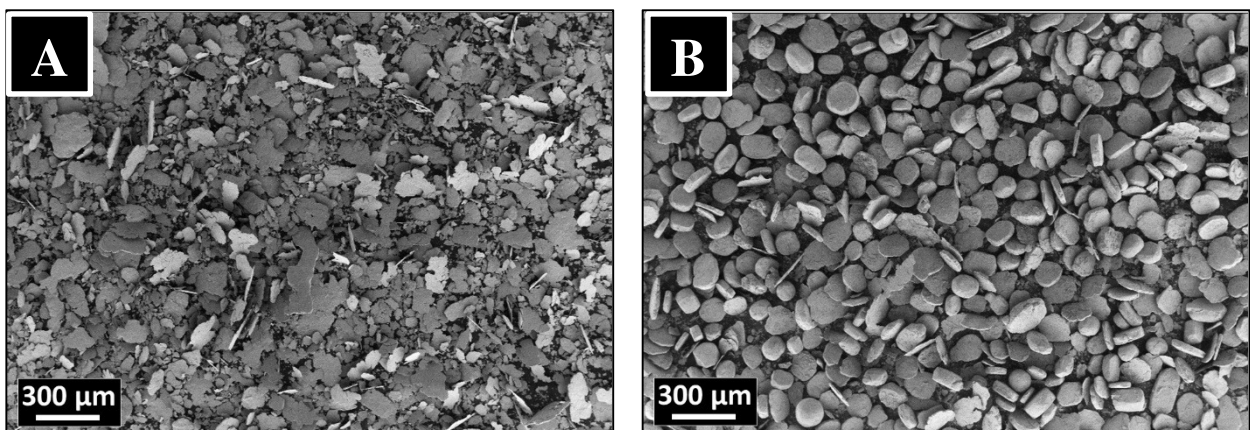


Fig. 4. SEM images of the milled 316L /Si<sub>3</sub>N<sub>4</sub>, A) 316L/0.33 wt% Si<sub>3</sub>N<sub>4</sub>, B) 316L/1 wt% Si<sub>3</sub>N<sub>4</sub>

### 3.2. Phase analysis of powder mixtures

Fig. 5 shows the XRD diffractograms of powder mixtures. The amount of ceramic additions in the case of 0.33 wt% composites (Fig. 5A) was under the detection limit. The phase analysis confirmed that the Höganäs 316L SS is austenitic of  $\gamma$ -Fe<sub>3</sub>Ni<sub>2</sub> phase (JCP2:03-065-5131) with main lines of ( $2\theta= 43.532^\circ, 50.705^\circ, 74.535^\circ$ ). Ferrite  $\alpha$ -Fe phase (JCP2: 03-065-4899) with main lines of ( $2\theta= 44.663^\circ, 65.008^\circ, 82.314^\circ$ ) has been observed after milling in the case of the SiC and Si<sub>3</sub>N<sub>4</sub> additions (Fig.5A) which might be a contamination from the milling setup (tank, balls, agitator). The high peak at  $2\theta= 69^\circ$  is the Si peak from the sample holder used during the XRD measurement.

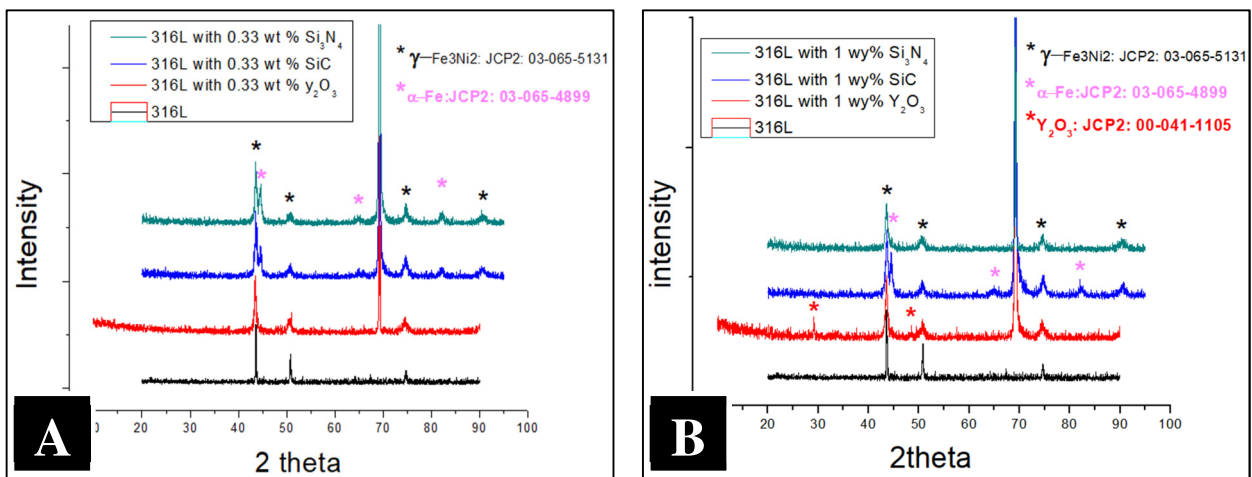


Fig. 5. XRD diffractogram of the milled powder mixtures in comparison with the 316L ss A) 0.33 wt% powders, B) 1 wt% powders

The added ceramic amount of the 1 wt% (Fig. 5B) was also under the detection limit of the XRD except in the case of 1 wt% Y<sub>2</sub>O<sub>3</sub> where two peaks have detected (JCP2: 00-041-1105) with the lines of ( $2\theta=29.150^\circ, 48.541^\circ$ ). The ferrite  $\alpha$ -Fe phase (JCP2: 03-065-4899) with main lines of ( $2\theta= 44.663^\circ, 65.008^\circ, 82.314^\circ$ ) have been observed also after milling in the case of the SiC and Si<sub>3</sub>N<sub>4</sub> additions (Fig. 5B).

### 3.3. Investigation of the ceramics distribution

The EDS spectra on Fig. 6 confirmed the composition of the 316L stainless steel provided by the manufacturer. The EDS spectra on Fig. 7A was taken from the selected zone on the inserted SEM image. The zone 1 (Fig. 7A) is the stainless steel matrix as it is confirmed by the EDS spectra, the Y<sub>2</sub>O<sub>3</sub> is embedded in the surface in dark spots form (zone 2 Fig. 7A), the lower intensity peaks of Fe and Cr and higher content of Oxygen is attributed to the good coverage of Y<sub>2</sub>O<sub>3</sub>.

Ben Zine H.R, Balázs C., Balázs K, *Anyagok Világa (Materials Word)* 1 (2018) 36-43

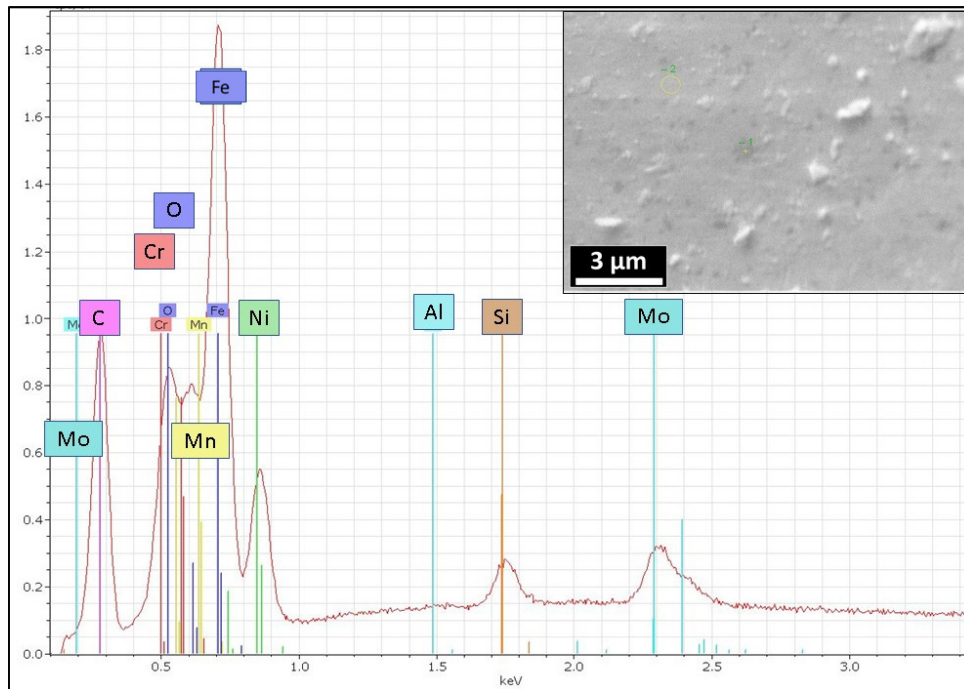


Fig. 6. 316L Reference EDS

The higher intensity of the Yttrium and Oxygen peaks (Fig. 7B) shows the better coverage and homogenous distribution of the  $Y_2O_3$  particles in the case of the 316L/1 wt%  $Y_2O_3$  composite.

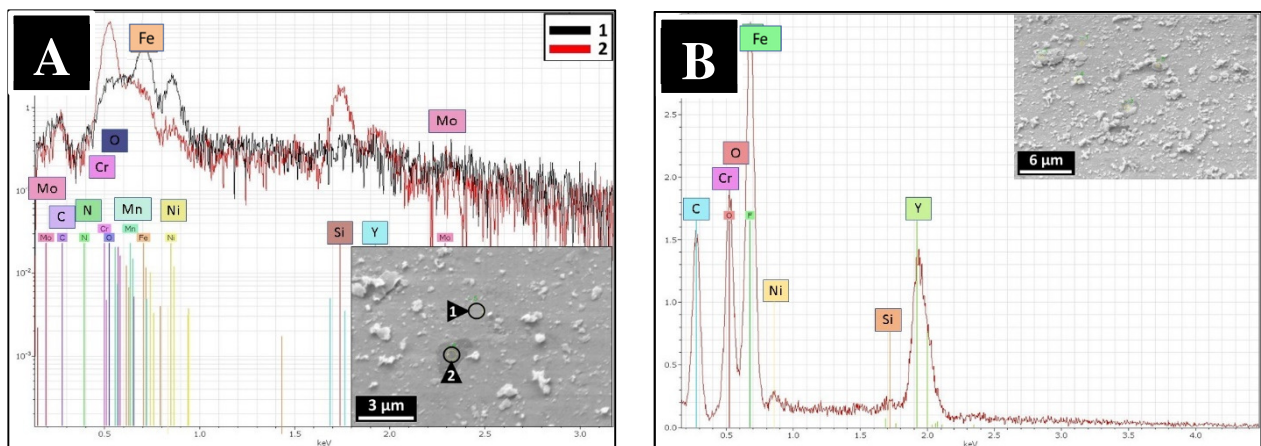


Fig. 7. EDS A) 316L/0.33 wt%  $Y_2O_3$ , B) 316L/ 1wt%  $Y_2O_3$

Ben Zine H.R, Balázsi C., Balázsi K, *Anyagok Világa (Materials Word)* 1 (2018) 36-43

EDS spectra of the 316L/SiC powder mixtures, specifically on surface of the grains are shown in Fig. 8. . The presence of the SiC is very clear in the dark zones 2 and 3 on the inserted SEM of Figure 8A, where the zones 1, 4 and 5 shows the steel matrix with very small amount of Silicon, the lower intensity peaks of Ni, Cr and Fe in the dark zones 2 and 3 shows the good coverage of the SiC.

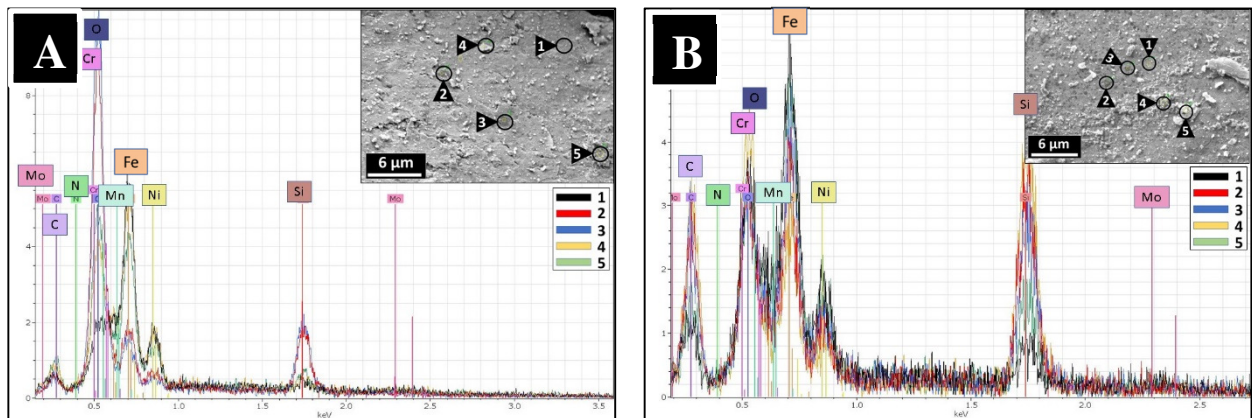


Fig. 8. EDS A) 316L/0.33 wt% SiC, B) 316L/ 1wt% SiC

More and homogenously distributed dark spots have been observed on the grains surfaces in the case of the 316L/1 wt% SiC due to the higher amount of SiC as it is confirmed by the EDS spectra in Fig. 8B. Similar embedded dark spots on the steel grains surface have been observed in the case of the 316L/Si<sub>3</sub>N<sub>4</sub> powder mixtures as it is shown in Fig. 9.

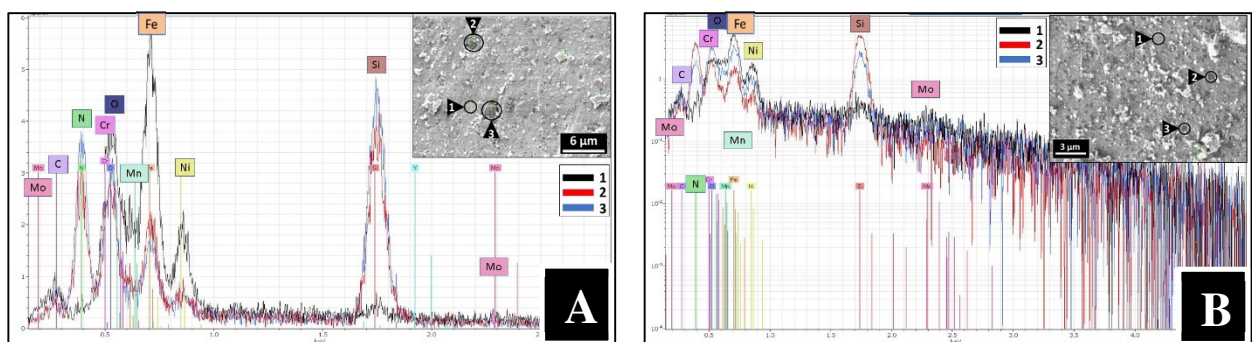


Fig. 9. EDS A) 316L/0.33 wt% Si<sub>3</sub>N<sub>4</sub>, B) 316L/ 1wt% Si<sub>3</sub>N<sub>4</sub>

#### 4. Conclusions

The effect of the different ceramic additives such as SiC, Si<sub>3</sub>N<sub>4</sub> and Y<sub>2</sub>O<sub>3</sub> on the morphological properties of 316L Stainless Steel have been studied during attrition milling process. Six different powder mixtures have been prepared with the compositions of

316L/0.33wt% and 316L/1wt% of the ceramic additive. The phase analysis confirmed that the Höganäs 316L SS is austenitic of  $\gamma$ -Fe<sub>3</sub>Ni<sub>2</sub> phase. Ferrite  $\alpha$ -Fe phase has been observed only after milling in the case of the SiC and Si<sub>3</sub>N<sub>4</sub> additions. Enhanced morphological changes and homogenous distribution of the ceramic particles in the steel matrix have been achieved in most cases.

### Acknowledgment

The authors would like to thank to Dr. Z.E. Horváth, Dr. Ákos Horváth (MTA EK) and L. Illés for their great contribution to this work.

### References

- [1] C. Suryanarayana and Nasser Al-Aqeeli, Mechanically alloyed nanocomposites, *Progress in Materials Science* 58 (2013) 383–502
- [2] H. Oka et al, Effects of milling process and alloying additions on oxide particle dispersion in austenitic stainless steel, *Journal of Nuclear Materials* 447 (2014) 248–253
- [3] C. Keller et al, Influence of spark plasma sintering conditions on the sintering and functional properties of an ultra-fine grained 316L stainless steel obtained from ball milled powder, *Materials Science & Engineering A* 665(2016)125–134
- [4] B. Al Mangour et al, In situ formation of TiC-particle-reinforced stainless steel matrix nanocomposites during ball milling: Feedstock powder preparation for selective laser melting at various energy densities, *Powder Technology* 326 (2018) 467–478
- [5] C. Tan et al, Investigation on 316L/316L-50W/W plate functionally graded materials fabricated by spark plasma sintering, *Fusion Engineering and Design* 125 (2017) 171–177
- [6] C. Tan et al, Investigation on 316L/W functionally graded materials fabricated by mechanical alloying and spark plasma sintering, *Journal of Nuclear Materials* 469 (2016) 32-38
- [7] L. Jinlong et al, The effect of surface enriched chromium and grain refinement by ball milling on corrosion resistance of 316L stainless steel, *Materials Research Bulletin* 91 (2017) 91–97